

Design and Implementation of Electrokinetic Probes for Cartilage Diagnosis

by

Jeffrey H. Tsay

Submitted to the Department of Physics and Department of
Electrical Engineering and Computer Science
in partial fulfillment of the requirements for the degree of
Master of Engineering in Electrical Engineering

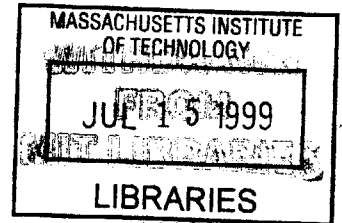
at the

MASSACHUSETTS INSTITUTE OF TECHNOLOGY

February 1999

© Jeffrey H. Tsay, MCMXCIX. All rights reserved.

The author hereby grants to MIT permission to reproduce and
distribute publicly paper and electronic copies of this thesis
document in whole or in part.



Author
Department of Physics and Department of Electrical Engineering
and Computer Science
February 3, 1999

Certified by
Alan J. Grodzinsky
Professor, Department of EECS, Mechanical, and Bioengineering
Thesis Supervisor

Accepted by
Arthur C. Smith
Chairman, Department Committee on Graduate Students

Design and Implementation of Electrokinetic Probes for Cartilage Diagnosis

by

Jeffrey H. Tsay

Submitted to the Department of Physics and Department of Electrical Engineering
and Computer Science
on February 3, 1999, in partial fulfillment of the
requirements for the degree of
Master of Engineering in Electrical Engineering

Abstract

In this thesis, piezoelectric laminate structures were designed and implemented to inject current into cartilage and measure the resulting stress, thereby diagnosing the material properties of the cartilage matrix. The laminate structures have undergone several design iterations and much work was done specifically with the class of laminate structures designed for hand-held in vivo probing of cartilage. The main focus of this project involved characterizing the overall variability of the probe system and attempting to understand issues which prevent the optimization of the data acquisition system.

Thesis Supervisor: Alan J. Grodzinsky

Title: Professor, Department of EECS, Mechanical, and Bioengineering

Acknowledgments

To begin, I would like to acknowledge all of the good people I've had the good fortune to meet over the past five-and-a-half years. While not all of you have had a direct influence on my work on this project, it is you who have helped shape me into the person I am today, and in so doing indirectly supported me through my time working on my thesis. For this, I am eternally grateful, and I thank you all.

My first round of acknowledgements must be given to the members of my lab. First and foremost, I must thank Alan Grodzinsky, who is undoubtedly the most well-spoken and diplomatic gentleman and mentor that I have ever met, and who will always serve as a source of personal and professional inspiration for all those he encounters. Next, I must thank Eliot Frank, from whom I believe I've learned more about real-life electronics than from all my other Course VI courses combined. And of course I must thank Steve Treppo and Emerson Quan, the Dynamic Duo of the Probesters, for all they've done for me. Thanks especially to Emerson, who was kind enough to share much of his own thesis work with me. Another word of thanks to Peter Gamache, for his contributions to Labview and to whom I give my best wishes for the remainder of his stay at MIT. Finally, my thanks to all the remaining members of the lab, for always making me feel right at home.

My second round of acknowledgements must be given to all the other MIT people who have helped me along for this project. Thanks to Dave Breslau, MIT machinist extraordinaire, for helping with the machining of hhv5.0 every once in a while. Thanks also to Joe Paradiso at the MIT Media Lab, whose interest in this project and expertise in piezoelectric films was and hopefully will be of much use to those who continue forward with this project. And thanks finally to Nelson Kiang, whose frank honesty always helped keep me in line with my own Truth.

My third round of acknowledgements must be given to the old gang from Emmaus, whose support and willingness to lend an ear for all my problems helped me over the

years in more ways than I can count. Thanks to Drew, my best buddy (even after all these years, if you can believe it), whose shoulder I've leaned on more than once. Thanks to Ian, my second best buddy, whose own dreams helped keep mine alive. May our annual Christmas get-togethers last for many, many years to come.

My final expressions of gratitude must be given to my family. Thanks to my Mom, Dad, and sister Jen, who really didn't have much of an idea what the hell I was doing on this project, but gave words of support regardless. And lastly, my thanks to beloved Sharon, who above all kept me sane and kept me safe all these years. Words cannot possibly describe my gratitude.

Contents

1	Introduction	7
2	Probe Structure and Circuitry	15
2.1	Basic Structure	16
2.1.1	Probe Laminate Structure	16
2.1.2	Version V (hhv5.0) Probe	17
2.1.3	Probe Versions and Fundamental Differences	20
2.2	Peripheral Circuitry	21
2.2.1	Electrometer	21
2.2.2	Lowpass Filters	22
3	Probe Fabrication and Design Issues	24
3.1	Probe Fabrication	24
3.1.1	Assembly	24
3.1.2	Photolithography	25
3.1.3	Etching	26
3.2	Design Issues	26
3.2.1	Capacitive Cross-talk	26
3.2.2	Variability	30
3.2.3	Signal-to-Noise Ratio	31
4	Experimental Methods and Results	34
4.1	Calibration	34

4.2	Experimental Procedure	37
4.3	Validation Experiment	39
5	Summary and Discussion	44

Chapter 1

Introduction

Osteoarthritis (OA) can be defined as a condition of synovial joints characterized by cartilage loss and evidence of accompanying periarticular bone response [3]. Typical symptoms include pain, stiffness, and limitation of motion for affected joints. OA is the most wide-spread disorder of diarthroidial joints that affects man. This condition tends to affect the older segment of the population, with the percentage of Americans over 65 years of age being the fastest growing segment. The rate of frequency of OA increases progressively so that in individuals of either sex over age 75, OA is an almost universal condition [5].

While OA is a condition of older populations of patients, the belief that OA is an inevitable disease of aging is both simplistic and inaccurate [8]. As the understanding of OA has deepened through scientific and clinical research, it has become clearer that OA is more a collection of degerative processes than a single clear-cut disease. This fact has resulted in some difficulties in studying OA, including a lack of a clear definition of the condition and a lack of agreed diagnostic criteria for OA. Currently, it is not clear exact what factor(s) lead to the development of OA. Racial and hereditary dispositions may have some affect on the issue, as well as obesity [8], but these general trends are not strongly correlated for all cases of OA. In fact, OA appears to be triggered by diverse constitutional and environmental factors which can vary widely.

As with any debilitating condition, steps to both treat and prevent the condition have been taken by the scientific and medical community. While a great deal of literature is available on the subject of OA treatment, there is relatively less literature concerning quantitative methods of early diagnosis of OA. The focus of this thesis is specifically in this arena of diagnosis in the spirit of OA prevention. In particular, this text describes the design and implementation of an instrument that can assess the electromechanical properties of cartilage. This capability serves the ultimate goal of allowing clinicians to semi-invasively probe articular cartilage and arrive at a quantitative diagnosis of the health of the cartilage in vivo.

Before detailing the workings of this diagnostic tool, it is useful to summarize some issues relating to the design and implementation of this instrument. This chapter first reviews the composition and behavior of articular cartilage, the material that is to be diagnosed. This section is followed by a summary of typical procedures that are currently available for treating OA cartilage and diagnosing cartilage, and concludes with a justification for the usefulness of the electromechanical diagnostic tool that is the focus of this project.

Hyaline cartilage is a term which describes a range of cartilaginous tissues noted for both resilience and mechanical durability under various loading conditions. Articular cartilage (AC) is a type of hyaline cartilage that is aneural, avascular, and alymphatic, and which covers the articulating surface of all diarthroidial joints. At a macroscopic level, AC appears as a translucent white material with a homogenous slick white surface. AC serves several functions, including:

- providing covering material to protect bone from abrasion and other damage,
- transmitting/distributing high compressive loads and shearing forces to subchondral bone,
- providing for joint congruity and maintenance of low contact stress between opposing bones, and

- providing a smooth lubricated surface that facilitates movement with little friction between articulating surfaces [9].

In this last function, healthy AC performs extraordinarily well, with cartilage on cartilage friction less than that of ice on ice [7].

While AC appears to be a homogenous, primitive tissue on the macroscopic level, inspection on the cellular level reveals distinct inhomogeneities in the tissue. In humans, the structure of adult AC is divided into roughly four different zones, beginning at the articulating surface of the cartilage and ending at the boundary between cartilage and subchondral bone. At an even finer scale, cartilage at the molecular level is composed of a hydrated gel matrix containing long cross-linked molecular chains of collagen fibrils and sulfated proteoglycans (PGs).

The relative molecular composition varies within the four different zones of the cartilage. The first zone, known as the superficial zone, is a thin, gliding surface with high collagen and low PG content. The second zone, known as the transitional zone, contains larger collagen fibrils and a higher concentration of PGs. The third zone, known as the deep zone, has the highest PG content and lowest water concentration of the four zones. The fourth and final zone is composed of calcified cartilage formed from mineralized cartilage matrix. The final zone delineates the separation of AC from subchondral bone [7].

While these zones help illustrate the fact that articular cartilage is highly organized rather than primitive tissue, it is the molecular interactions of the AC matrix its components that ultimately determine the behavior of the cartilage as a whole. At the this level, AC consists of chondrocytes and extracellular matrix (ECM) (Figure 1-1). Chondrocytes make up less than five percent of the total tissue volume and are characterized by their small size and generally rounded appearance. ECM rounds out most of the remaining tissue volume and is composed of the sulfated PGs and collagen, which are principally type II crosslinked with type IX collagen fibrils. These

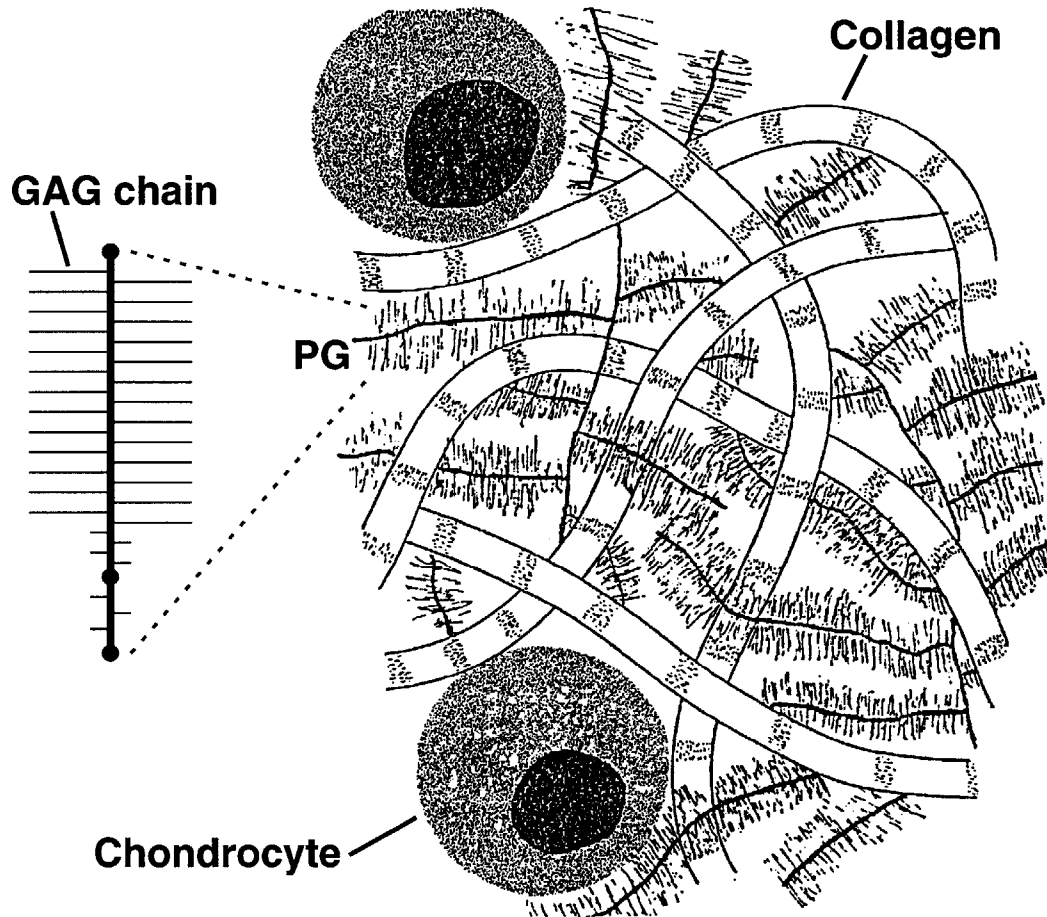


Figure 1-1: Components of articular cartilage.

two basic components complement each other in order to maintain the healthiness of the tissue. The small but important population of chondrocytes plays a crucial role in the production, organization, and maintenance of the ECM, while the ECM in turn protects the chondrocytes from damage from external mechanical loads [9]. The PGs have a high concentration of negative fixed-charge sulfate groups. The electrostatic repulsive forces between these strands of PGs determine the high compressive stiffness of AC. In contrast, the collagen network determines the tensile properties of the ECM and AC overall [6]. The action and interaction of the overall network of PGs and collagen is the key to the resiliency that AC is known for.

In addition to natural aging processes, direct physical damage from external injuries can also induce OA. In particular, injuries that do not extend to subchondral bone and its vasculature have the lowest self-healing capacity, because the bone cannot mount an inflammatory response. In cases where repair can and does occur, the repair tissue initially consists predominantly of type I collagen, typical of fibrocartilage. Over a time span of up to 24 months, the type II collagen associated with the repair tissue may increase, making the tissue increasingly hyaline. However, after roughly 24 months, the repair tissue typically splits and fibrillates, resulting in changes not dissimilar to that seen in OA. Over the lifespan of the repair tissue, type I collagen remains a significant presence, suggesting that normal hyaline cartilage never develops at these repair sites. Thus, typical repair by fibrocartilage tends to deteriorate over a matter of several months and ultimately result in symptoms similar to that of OA [7].

There are currently a number of medical treatments and surgical procedures which attempt to mitigate the symptoms of OA, whether from old age or physical injury. These procedures can be categorized as trying to either treat symptoms or effect repair. Some of the tissue repair procedures result in the stimulation of fibrocartilage as a substitute repair tissue, but as discussed above, this type of repair tissue lacks durability and typically degenerates over time. In general, these surgical procedures

are partially successful in temporarily reducing pain and increasing mobility, but no one procedure has been totally successful in achieving regeneration of normal articular cartilage [7].

While much effort has gone into treating victims of OA, relatively less work has been done in the area of diagnosis and prevention of cartilage degradation. During such procedures as arthroscopy, a surgeon can make a visual assessment of the health of cartilage, but this is both qualitative and inaccurate in terms of determining the true health of the ECM and chondrocytes of a given portion of cartilage tissue. However, it is difficult to gain any quantitative information about the condition of cartilage tissue without being invasive and potentially damaging the cartilage.

One example of a semi-invasive diagnostic tool which is currently commercially available is a mechanical indenter probe by Lyyra et. al. [6]. The indenter probe was designed to obtain an instantaneous in vivo measurement of cartilage stiffness. Because among the first changes during cartilage degradation are an increase in amount of interstitial water, and a decrease in the content and aggregation of PGs, this results in an overall softening of cartilage tissue. Thus, the indenter probe provides a mechanical quantitative measurement of the relative structural health of cartilage relative to a calibrated baseline of other normal healthy tissue.

While this example of a diagnostic tool does provide a semi-invasive quantitative measurement of a mechanical property of cartilage which can be correlated to the structural health of the tissue, this tool does have some drawbacks. One design drawback is that in order to determine an actual value for the cartilage, the thickness of the cartilage tissue at the point of acquisition needs to be known, and there is currently no practical method for obtaining this metric. The indenter probe attempts to make the measurement as independent as possible from the thickness of the tissue by making the dimensions of the indenter as small as possible relative to the thickness of the tissue. However, as the thickness of the tissue approaches 1 mm and below (which is not unreasonable in various areas of the human knee, for instance), this

approximation loses its validity.

Another major drawback of the indenter probe is that the measurement itself does not take into account the fact that cartilage has both electrical and mechanical material properties. A measurement which incorporates both of these issues might reflect more accurately the state of the cartilage being probed. Such a measurement does exist, and involves the application of voltage across cartilage matrix in order to induce mechanical stress. This electromechanical property of cartilage allows a coupling of electrical and mechanical stimuli, and leads the way to a measurement of current-generated stress of cartilage. In current generated stress, a voltage applied across cartilage matrix causes the PG strands with their high density of negative fixed-charges to be attracted to the positive electrode, while the free-floating positive ions in the hydrated matrix are attracted to the negative electrode (Figure 1-2).

Current generated stress can be performed with electrodes located on opposite sides of cartilage matrix, but can also be performed with electrodes placed on the same side of the matrix [11, 10]. This technique has been termed electromechanical surface spectroscopy and is the basis for the probe presented in the rest of this thesis. Unlike the purely mechanical indenter probe, this electromechanical diagnostic tool is capable of taking advantage of the fundamental electromechanical property of cartilage in its measurement of current generated stress. Furthermore, quantitative measurements from current generated stress can be used to determine parameters of cartilage material properties based on mathematical models [10], ultimately providing a direct measure of cartilage matrix health.

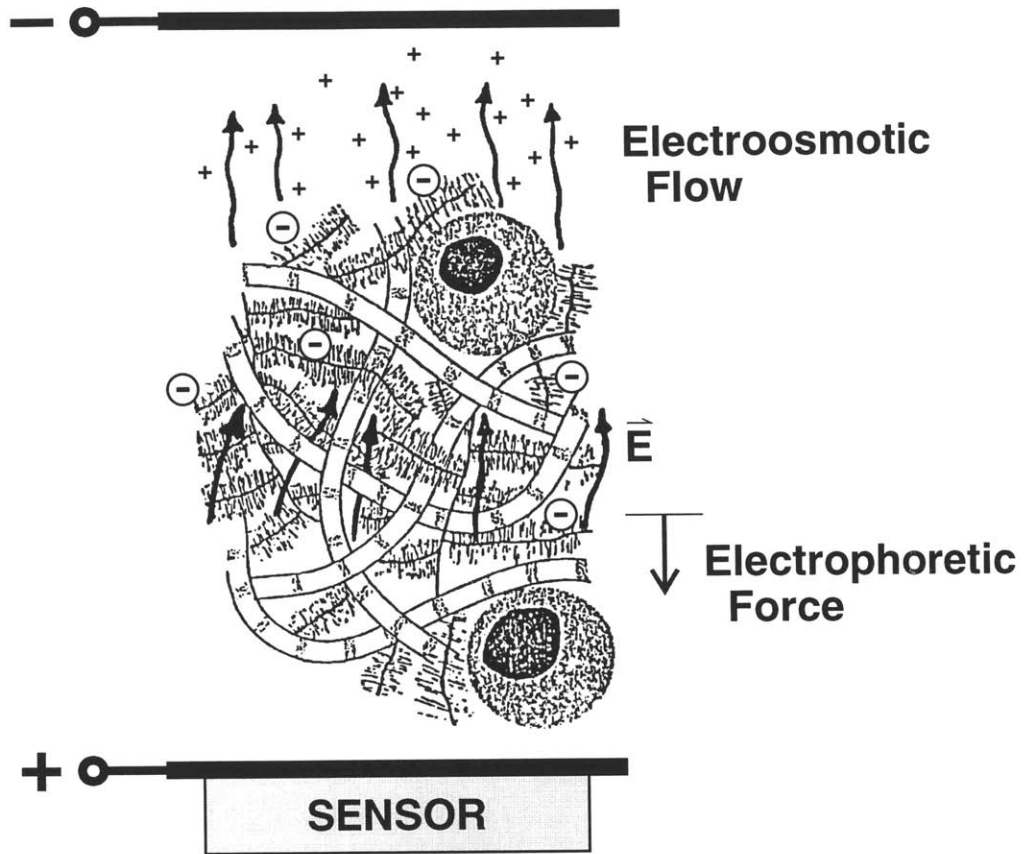


Figure 1-2: Current generated stress.

Chapter 2

Probe Structure and Circuitry

The term “probe” used throughout this text refers in general to a class of three-layer laminate structures mounted in a hand-held structure that applies an input current to cartilage and measures an output load. While this aspect of the probe project is concerned specifically with the most recent version of the probe intended for use *in vivo*, there are a number of different *in vitro* versions of the probe as well [1, 13]. Although details of the design and implementation of the *in vitro* series will not be directly addressed, it will be useful to compare the *in vivo* series to the *in vitro* series in order to appreciate some of the issues considered during design.

Before going into the physical details of the various versions of the probe, some terminology issues should be addressed. The first broad category of probes are the *in vitro* probes, also commonly referred to as “bench-top” probes, and were historically the first probes to be designed, fabricated, and tested. As the name suggests, these probes were and still are used to probe cartilage discs in an *in vitro* situation. The second broad category of probes are the *in vivo* or “hand-held” probes, and represent a step towards making these probes more applicable to an *in vivo* setting as one finds in arthroscopy. Under this more recent category exist two series of probes and are commonly referred to as the version IV and version V hand-held probes. In this text, these two series of *in vivo* probes will be abbreviated as hhv4.0 and hhv5.0 respectively. The version numbers indicate the design iteration which produced each

series, and thus hhv5.0 is currently the most recent addition to the probe family.

2.1 Basic Structure

2.1.1 Probe Laminate Structure

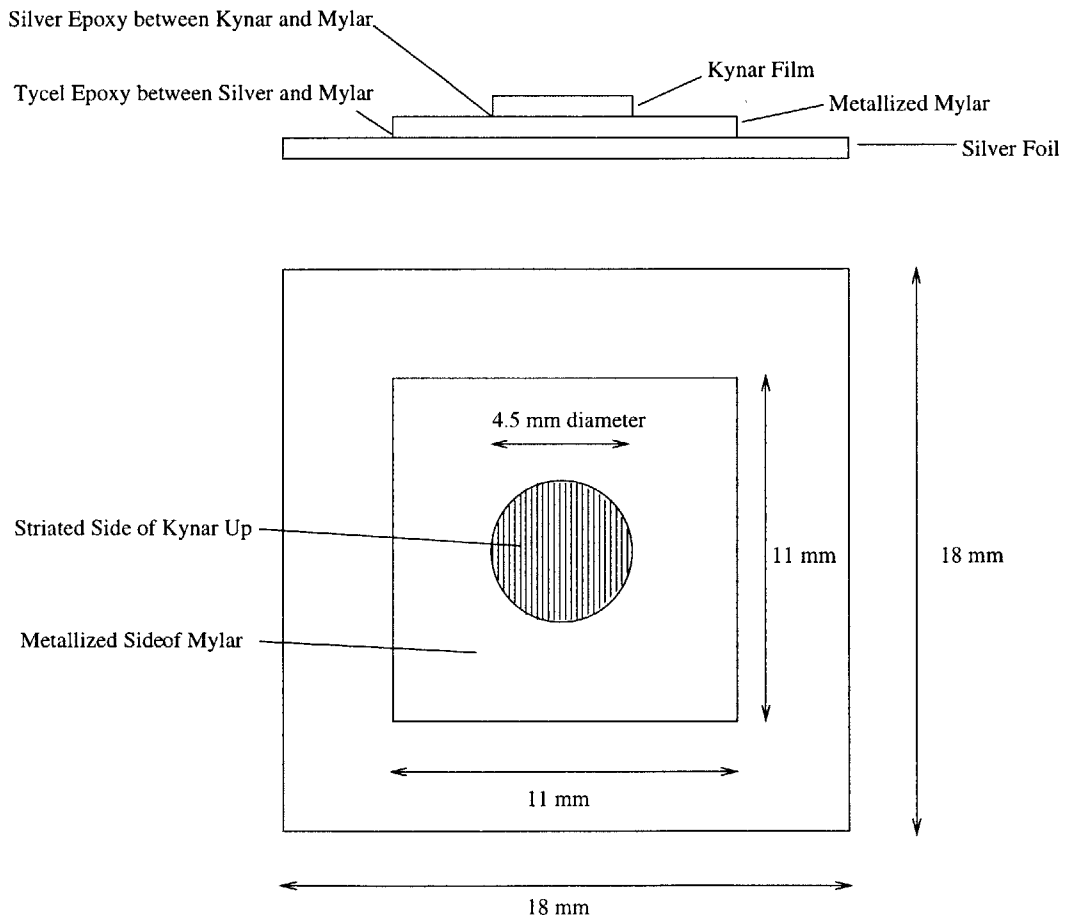


Figure 2-1: 3-Layer Laminate Structure of hhv5.0

The active area of the probe is a multi-layered laminate structure and is shown above (Figure 2-1). The silver electrodes deliver the input current into the cartilage extra-

cellular matrix. The silver electrodes are bonded to the a layer of Mylar polyester with a two-part urethane epoxy. The Mylar has a sputtered aluminum coating on one side which acts as a ground plane and shields the output electrodes from the input electrodes. The Kynar piezoelectric polyvinylidene fluoride (PVDF) film is bonded to the Mylar ground plane with a conductive silver epoxy in order to ensure an electrical connection between the ground plane and one side of the Kynar film. The Kynar film itself is also sputtered on both sides with a nickel/copper alloy. The patterns on the non-bonded side of the Kynar are used as the output electrodes of the probe structure. The Kynar film outputs a voltage in proportion to the pressure exerted by the cartilage in response to the input current.

2.1.2 Version V (hhv5.0) Probe

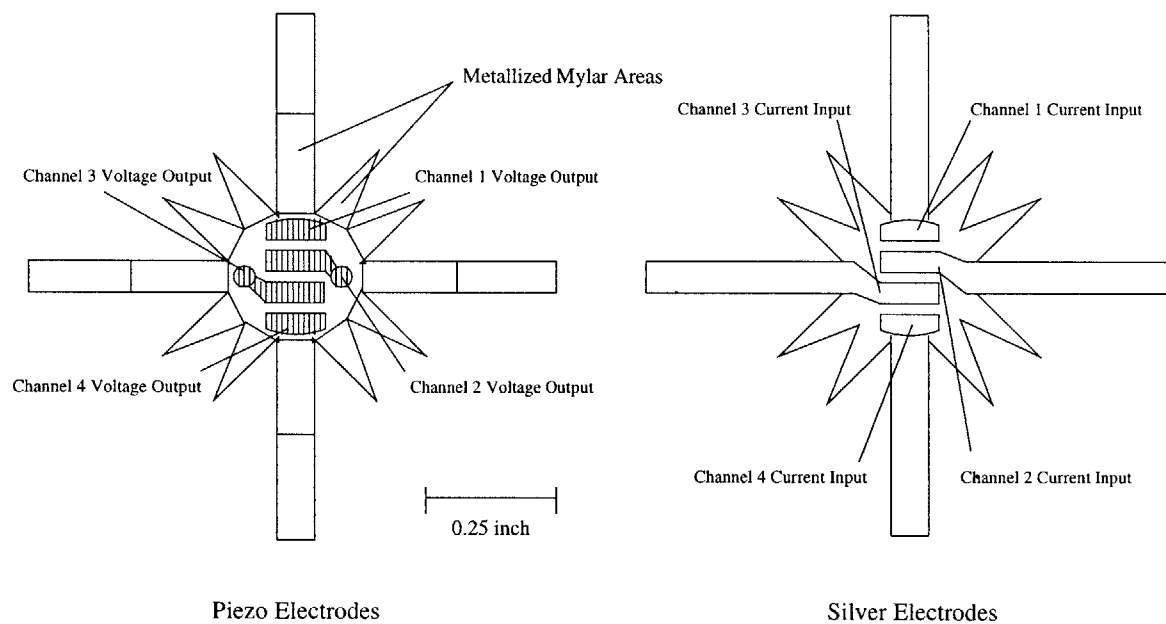


Figure 2-2: Input and Output Electrodes for hhv5.0

Probe Electrodes

The input and output electrodes for the hhv5.0 probes are shown above (Figure 2-2), with the input electrodes on the right and the output electrodes inside the circular border on the left. The input and output electrodes are fabricated so that they line

up precisely with one another. The fact that there are four input electrodes allows the probe to apply different current patterns to the cartilage matrix. These different current patterns result in different spatial distributions of current density within the cartilage matrix.

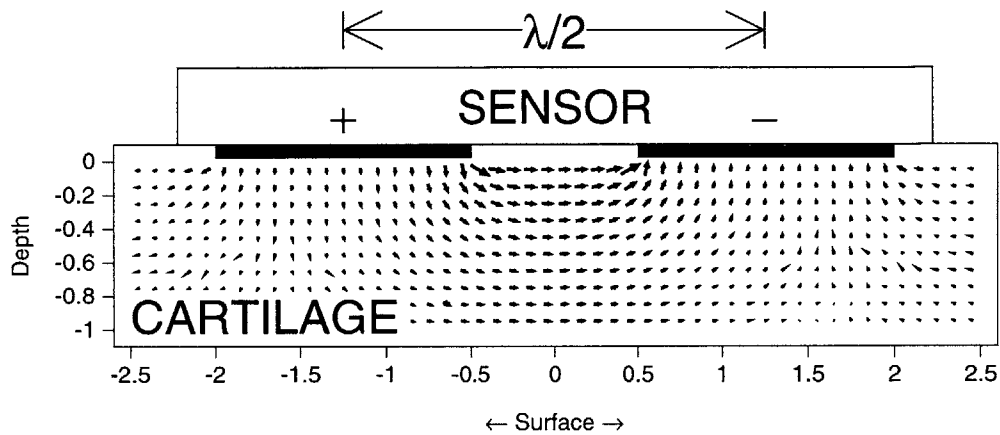


Figure 2-3: Spatial current distribution for a two-electrode probe.

A depiction of the intratissue current density distribution for a two-electrode probe is shown above (Figure 2-3). This flexibility allows the user to effectively probe varying depths within the cartilage matrix.

Probe Core, Sheath, and Outer Body

The insulating sheath and stainless steel inner core and outer body are shown below (Figure 2-4). The outer body encases the sheath, probe laminate structure, and inner core. The core is composed of several parts and is responsible for making the electrical connections to the silver input electrodes and to the Kynar output electrodes. The input electrodes are press-connected to copper tabs at the outer cylindrical surface of the core, which are connected by thin wires to the input plugs. The output electrodes are press-connected to brass contacts on the circular face of the core, which are in turn soldered to the wires of a four-conductor cable terminating at a female BNC connector. The insulating sheath fits over the probe laminate structure and ensures

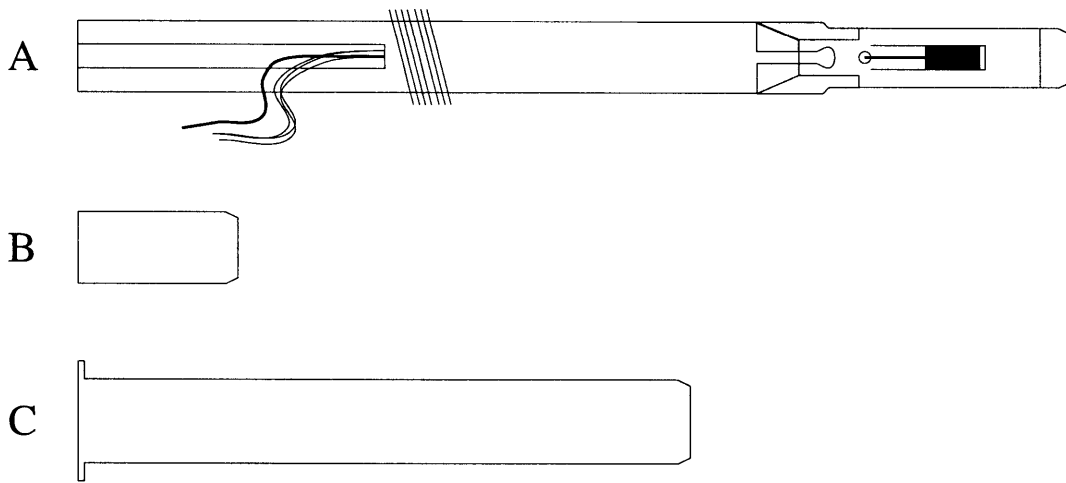


Figure 2-4: The three parts of hhv5.0. A: Inner core, B: Insulating sheath, and C: Outer body.

good contact between the input and output electrodes of the inner core and probe laminate structure.

2.1.3 Probe Versions and Fundamental Differences

Although the basic laminate layer structure is the same for both the *in vitro* and *in vivo* probe series, the shape and patterns of the probes structures are quite different. For the *in vitro* series, the probe structures are designed to accomodate cartilage discs which have been harvested from freshly slaughtered cows or calves. These discs are generally 9 mm in diameter, and are much wider than the $\frac{1}{4}$ " diameter apertures which are typically available in arthroscopic *in vivo* settings. This allows the *in vitro* probes a larger active surface area.

Another major physical difference between the *in vivo* and *in vitro* probes is that the input and output sides of the probe structures are kept physically isolated through different means. The *in vitro* probes are mounted in a chamber which fits together to expose only the necessary active input area of the probe structure. A rubber O-ring delineates the edge of the active area and prevents any fluid from seeping to the output side of the structure. In contrast, the *in vivo* probes are sandwiched between a stainless steel body and core. The core presses the structure against the lip of the sheath, leaving only the silver electrodes exposed to the outside environment. To prevent fluid from seeping into the body of the probe, a RTV silicone sealant is applied between the lip of the sheath and the outer periphery of the active output area. This distinction becomes important when considering possible design issues for the *in vivo* probes, because the RTV sealant is far less reliable than the O-ring in terms of keeping out fluid.

Finally, one major distinction between the hhv4.0 and hhv5.0 series of *in vivo* probes is that the number of electrodes is different. The older hhv4.0 has one pair of input and output electrodes, while the newer hhv5.0 has two pairs of input and output electrodes. As discussed above, the extra pair of electrodes gives the hhv5.0 flexibility

over the depth of current penetration into the cartilage matrix, and consequently allows the probe to assess the mechanical properties of different levels within the matrix.

2.2 Peripheral Circuitry

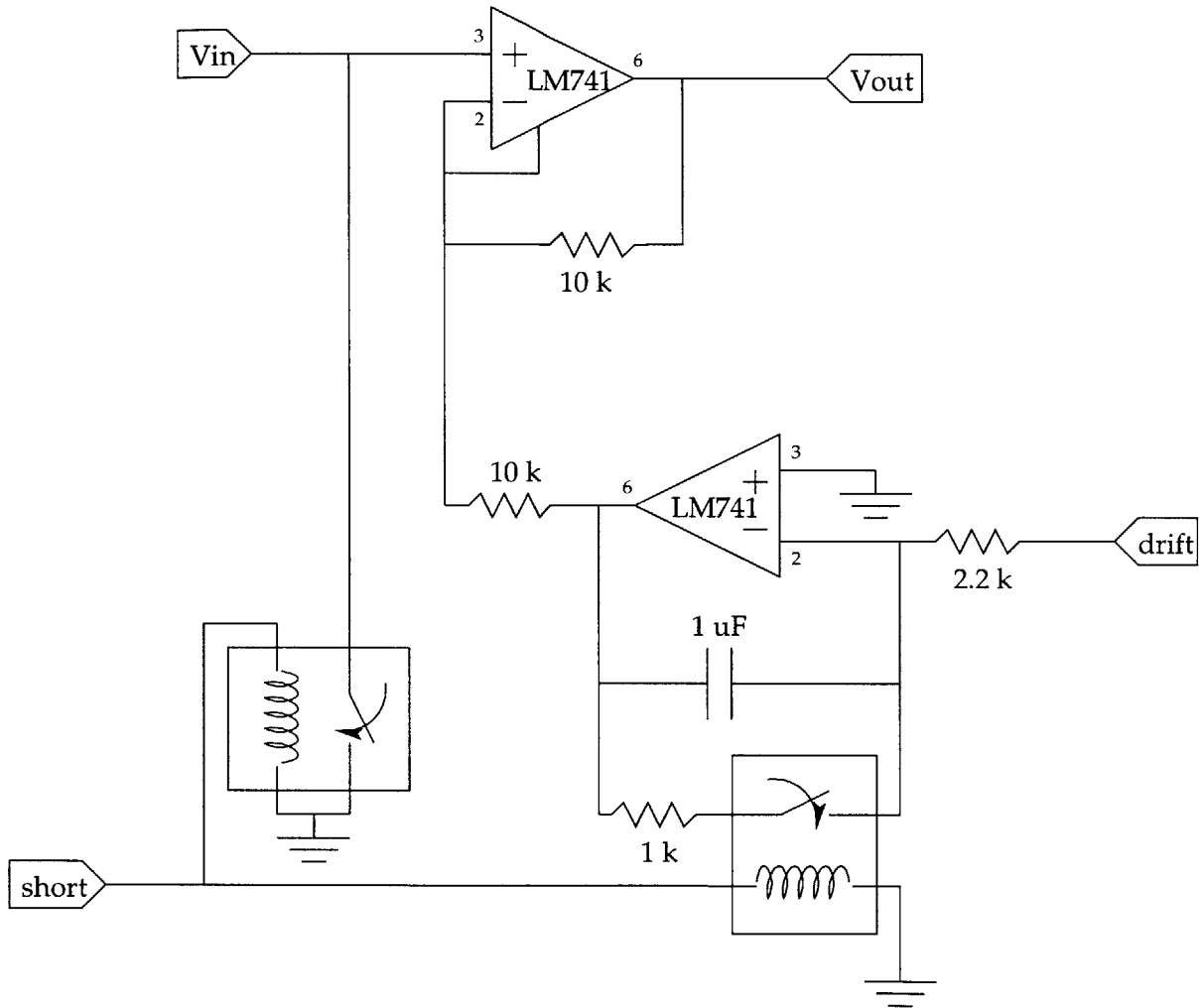


Figure 2-5: Circuit diagram for a single channel electrometer.

2.2.1 Electrometer

The outputs from both *in vivo* and *in vitro* probes are connected directly to the input of the electrometer. The electrometer essentially consists of two stages of op-amps (Figure 2-5). The output of the probe is fed to the input of the first op-

amp stage, which acts as a simple voltage buffer and converts the signal from high impedance to low impedance. The second op-amp stage is an integrator, with a manually adjustable DC voltage as its input. This stage serves to add a linear voltage component to the probe output voltage, which allows the probe user to zero the output voltage, a capability which is essential during calibration and experimentation, and which is referred to as drift control.

Because hhv5.0 is a 4-output device, the electrometer must also be able to support four channels simultaneously. Since the previous hhv4.0 version only possessed 2 outputs, there has been a need for a new 4-channel electrometer to replace the old 2-channel electrometer. In addition to requiring a new electrometer, the current desire is to have the drift control automatically driven by the computer. Therefore, the newest version of the electrometer has been constructed with this purpose in mind. Although the conversion from using the hhv4.0 to the hhv5.0 is well underway, one obstacle which is rapidly approaching a resolution is the need for software which can simultaneously input and output four different voltage signals. The current aim is to implement these functions with the most recent student version of Labview, and is a goal which should soon be achieved.

2.2.2 Lowpass Filters

The electrometer signals travel directly to a set of lowpass filters which cut-off frequencies above 15.7 Hz. Again, with the current drive to upgrade from hhv4.0 to hhv5.0, there has been a need to replace the set of old non-portable 4-pole filters with a portable 2-pole active filter (Figure 2-6). These filters are hard-wired directly into the same hardware that houses the 4-channel electrometer, and the outputs of the electrometer are fed directly to the inputs of the lowpass filters. The filtered signals are then sent to the data acquisition board and are processed by the computer.

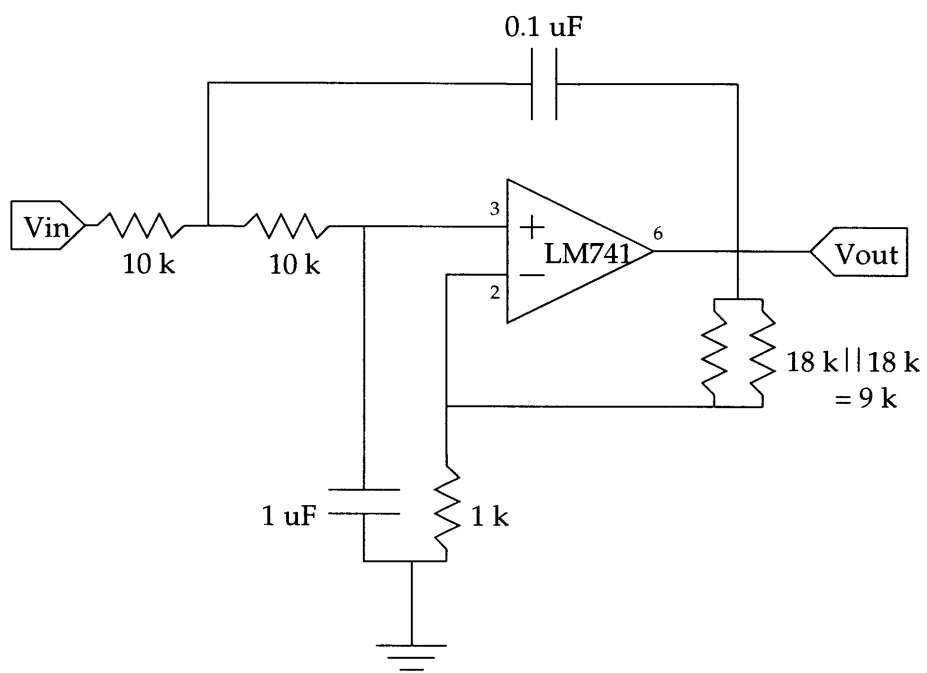


Figure 2-6: 2-pole low pass filter with cutoff frequency 15.7 Hz.

Chapter 3

Probe Fabrication and Design Issues

3.1 Probe Fabrication

The following sections discuss the methods and procedures used for manufacturing the probe laminate structures. As a general rule, each phase of the manufacturing protocol requires a day to complete. Because of the time intensive nature of this procedure, it is essential that all precautions are taken in order to maximize the yield of each run. Typically, probe structures are manufactured in batches of four or eight due to that fact that the masks used in the photolithography phase can only accommodate four probes each at a time. Therefore, the following discussions focus less on a comprehensive listing of all the fabrication steps and more on details essential for a successful manufacturing run.

3.1.1 Assembly

The process for constructing the probe structures begins with collecting one sheet each of silver, Mylar, and Kynar. Before cutting the necessary pieces from these sheets, it is important that the area of the silver sheet be abraded with fine emory or sand paper. Experience suggests that a granularity of at least 600 dpi be used for this

purpose, and that small circular strokes be used to ensure a smooth even distribution of the abrasion.

The other delicate steps in this stage of fabrication involve the two different types of epoxy used to bond the silver sheet and the Kynar film to the Mylar film. In both cases of the silver epoxy and the Tycel urethane epoxy, it is important to be as careful as possible to use precisely the right amount. Too little of either epoxy, especially the silver epoxy, may result in the probe structure delaminating during the course of fabrication. In the case of the Tycel, it is useful to know that it is possible to remove excess epoxy from the laminated structure by dipping a cotton-tipped applicator in the solvent used to dissolve the Tycel during its mixing and lightly brushing away the excess epoxy. In the case of the silver epoxy, any excess epoxy is in general very difficult to remove because the epoxy even in its uncured stage is somewhat viscous and will smear easily.

3.1.2 Photolithography

The photolithography stage is a delicate phase of the fabrication process. Two major keys to a successful photolithography run are to make sure that the dehydration cycles are as close to the suggested 10 minutes as possible, and that the oven temperature *does not exceed* 80 degrees. The Kynar film is very sensitive to temperature, and like any other plastic will shrink when exposed to too much heat. It is also important to make very certain that the photomasks and glass plates used for the exposing step are as clean and particle-free as possible, since even the smallest dust particle can introduce flaws into the patterns for the electrodes. From experience, it is not wise to use water to clean the photomasks (which then stick together). Instead, it is recommended that they be wiped down with Kimwipes, which are lint-free wipes available in the lab.

3.1.3 Etching

The etching phase is generally not a source for concern, as long as one takes care not to expose the aluminum metallization on the Mylar to any droplets of etchant. It is also wise not to apply too much developer to the silver electrodes when stripping off the photoresist, since this can result in the loosening of the epoxy bonding the silver electrodes to the Mylar.

3.2 Design Issues

The following sections attempt to characterize the design issues currently of interest to the hhv5.0 series of *in vivo* probes. While data collected by various versions of the probe in the past have supported theories and models of current-generated stress in cartilage, there are a number of design issues which prevent the probe from being a consistently reliable diagnostic tool. The discussions below attempt to describe some of these design issues and related observed phenomena, and to present some current theories and suggestions for addressing these issues.

3.2.1 Capacitive Cross-talk

In principle, the piezoelectric electrodes output voltage should be proportional to the normal mechanical stress induced at the cartilage/kynar interface by the input current. Conversely, it follows that the piezoelectric output voltage should be zero, ideally, when there is no cartilage pressing against the active probe face, *even* when there is an input current. Therefore, applying a sinusoidal input current into an electrolytic solution (e.g. NaCl in water) should not result in a correlated sinusoidal output voltage.

However, there have been several instances where the piezoelectric electrodes *do* output a sinusoidal voltage while the probe is immersed in a pure electrolyte. The effect has been seen intermittently, and has been observed in both versions of the hand-held probes. This phenomenon has been termed cross-talk, or sometimes capacitive

cross-talk, in keeping with the current theory for its cause. The most popular theory to date as to the cause of the cross-talk is that the piezoelectric output electrodes are not electrically shielded well enough from the silver input electrodes, resulting in a capacitive coupling between the input and output electrodes. Physically, this suggests that the ground plane created by the Mylar aluminum metallization bonded to the Kynar nickel/copper alloy metallization by means of the silver epoxy is not fully conducting, or that the plane itself does not sufficiently cover the piezoelectric electrodes themselves well enough.

However, it is instructive to state the known facts concerning past observed occurrences of cross-talk. First, most probes which have exhibited cross-talk behavior generally show little or no such behavior when they are first mounted into the probe sheath. Then, over the course of an experiment in which current is being injected into cartilage, a signal will begin to develop that appears sinusoidal, will tend to increase in magnitude with decreasing frequency of the input current, and will tend to have roughly a 90 degree phase lag with respect to the input sinusoid. Unfortunately, these characteristics can mirror normal expectations of what current-generated stress should look like, both in terms of magnitude and phase. There also seems to be a threshold effect: once cross-talk behavior occurs, it tends to remain, even given a few hours during which the probe is not being used.

Recent occurrences of the cross-talk have prompted further experimental study of this effect. Because the cross-talk seems to develop over time, it is unclear whether or not cross-talk develops gradually over time as the probe is used, or if there is some particular action or environmental factor that triggers the onset of cross-talk. To explore this, a hhv5.0 probe was tested for cross-talk in electrolyte for several runs, during and after which no observable cross-talk manifested itself. Naturally this suggests, but does not prove, that cross-talk may be triggered by some particular action or effect. Also from recent events, it has been observed that after the onset of cross-talk the calibration of the piezoelectric material no longer exhibits its normal

sinusoidal behavior, suggesting that there might be some sort of material property change associated with the cross-talk phenomenon. Additional investigation reveals a trend of increasing cross-talk with increasing static load on the probe face.

While the above anecdotal evidence highlights some of the more interesting characteristics of cross-talk behavior, it should be noted that the recent studies presented were only made with *one* particular hhv5.0 probe. Therefore, any light these trends might shed on the nature of cross-talk must be viewed under suspicion that the trends may in fact be specific to that probe alone.

As cross-talk is currently the major issue impeding the implementation of the probe, several attempts have been made to either understand the phenomenon or circumvent its effects. The discussion above illustrates some of the steps that have been taken to try to characterize the nature of cross-talk. However, one major limiting factor is the time-intensive nature of probe manufacturing. Even given a perfect manufacturing run that produces eight viable probe structures, the process of mounting a new probe takes at least a day in order for the sealant to cure. At the moment, probe manufacturing is still a custom crafting art form, and is therefore unfortunately not a process that lends itself to any sort of streamlined assembly line fabrication process. This leads into an issue of variability between probe structures. Because of the man-made nature of the probe manufacturing process, each probe tends to be at best slightly different than all other probes created, even in the same run. While human error may not ultimately be the major contributing factor, variability between probes is nevertheless another major issue that must be taken into consideration. With regard to the cross-talk phenomenon, this means that attempts to empirically study cross-talk should be done over a large pool of probes so that any specific probe-to-probe variations might be averaged out in the end. These two issues – time of manufacturing and mounting and the need for a large number of probes – make the task of studying the cross-talk phenomenon through experimentation problematic at best.

Another possible approach to dealing with cross-talk is simply to circumvent its effects by altering the probe design in some fashion. This approach assumes that the theory of capacitive coupling between the input and output electrodes accounts for all or most of the cross-talk phenomenon. There are different levels of alteration when considering the design of the probe. One drastic level of alteration is a complete redesign of the probe sheath, core, and structure, with the intent of shielding the output electrodes as thoroughly as possible. However, an undertaking of this level would require many weeks and possibly months of devoted time and effort, and is generally viewed as a last resort. A less drastic level of alteration involves optimizing the shielding that exists. The silver epoxy which conductively bonds together the aluminum metallization of the Mylar and the nickel/copper alloy metallization of the Kynar has in the past been somewhat suspect in that, upon disassembly of a number of past worn-out probes, the Kynar film fell apart from the Mylar film. This suggests that the silver epoxy may not be bonding as well as it should, and so there have been attempts at using different brands and formulations of silver epoxies. Currently, all the various types of silver epoxy that have been tried have their advantages and disadvantages, and none seems optimal. In addition, it is not clear whether or not the silver epoxy really is a significant issue since the Kynar theoretically should be pressed against the Mylar by the pressure of the probe core against the probe sheath, and so an electrical connection should still technically exist. However, a resolution to the silver epoxy issue, even if it did not eliminate the cross-talk problem, would at least eliminate one further variable of uncertainty in this system.

It cannot be overemphasized just how critical the cross-talk phenomenon is in regard to the overall project. Until it can be determined either how to prevent cross-talk from occurring or how to determine the amount cross-talk contributes to a given output signal, the cross-talk effect will continue to cast a shadow over the reliability of the probe as a diagnostic tool for cartilage.

3.2.2 Variability

For any diagnostic tool, it is important to address the issue of the variability in the behavior of the instrument. In the case of the *in vivo* versions of the probe, the slight physical differences of each probe due to the manufacturing process make variability that much more of a concern. In practical useage, one generally sees a great deal of variation in two areas: probe calibration and cross-talk.

The exact procedure used to calibrate each probe before every experiment is detailed in Chapter III. For both the hhv4.0 and hhv5.0 series of probes, the calibration numbers for each electrode on each probe tend to vary from probe to probe. In the case of hhv4.0, typical numbers for calibration tend to run from as low as 10 mV/kPa to as high as 60 mV/kPa, though most tend to be in the 20 to 30 mV/kPa. For hhv5.0, typical calibration numbers tend to run between 100 and 700 $\mu\text{V}/\text{kPa}$, averaging around 200 to 300 $\mu\text{V}/\text{kPa}$. It is comforting to note that for a single calibration setup, the calibration numbers do not vary significantly.

However, on a daily basis calibration numbers *have* been known to fluctuate by up to roughly 10 mV/kPa for hhv4.0 and roughly 50 to even 100 $\mu\text{V}/\text{kPa}$ for hhv5.0. Thus it is especially important to calibrate the probe at the beginning of each daily experiment. Calibration numbers (and signals) have also been known to fluctuate after the onset of cross-talk as described in the previous section, and it is therefore also important to attempt a calibration of the probe immediately after the conclusion of an experiment.

Also mentioned in the previous section is the uncertainty of how quickly (if at all) cross-talk occurs during an experimental run. While the onset has been observed to range over a wide timespan (minutes to hours), the magnitude and phase of the cross-talk signal has also been observed to vary quite a bit. As is described previously, upon the setting in of cross-talk, the magnitude of the cross-talk signal tends to grow inversely proportional to the frequency of the input current signal, while the phase has a general tendency to appear to lag roughly 90 degrees with respect to the input

signal. However, these are merely broad generalizations; there have been instances where the cross-talk magnitude seemed small and fairly constant as a function of frequency, while the phase under similar circumstances appeared to randomly vary over any number of degrees. It is important to note that in these instances, the cross-talk is often not easily recognizable apart from other sources of noise in the system such as the natural low-frequency voltage drift of the piezoelectric film, and will look very non-sinusoidal. This makes it very difficult to know exactly when cross-talk behavior is beginning to manifest itself in the system during an experimental run.

3.2.3 Signal-to-Noise Ratio

Another quantity useful for characterizing a system is the typical signal-to-noise ratio (SNR) of the output. In the case of the two hand-held versions of the probe, the SNR is significantly higher for hhv5.0 compared to that of hhv4.0. While the overall noise in the system does include sources introduced by the circuitry and connections between the probe and the computer, the major source of noise originates primarily from the low-frequency voltage drift of the piezoelectric material. The overall signal for a piezoelectric material is governed by

$$V = \frac{d_t \sigma \delta}{\epsilon} \frac{A}{A'}$$

where d_t is an empirically determined piezoelectric strain constant,

σ is a stress,

δ is the film thickness,

ϵ is the dielectric constant of the film,

A is the active area of the electrode being loaded, and

A' is the total electrode area.

Consequently, because hhv5.0 has output piezoelectric electrodes of smaller area compared to the larger hhv4.0, the pure signal is also of lower amplitude, resulting in

a lower SNR for hhv5.0 overall.

Experience with hhv5.0 suggests that it is possible to capture enough signal during an experiment even with the lower SNR. However, given the difficulties created by the cross-talk phenomenon, as well as normal variations from probe to probe in terms of calibration numbers, which are indicative of the useful output potential of each output electrode, there is constant concern with any newly mounted probe that it may be unable to generate enough signal to allow for a successful experimental run.

Attempts to address this particular design issue have focused more on boosting the useful signal from the probe rather than attempting to reduce the amount of noise from the system, simply because it is conceptually easier to do so. One suggested method is to increase the amplitude of the input current by a factor of two to three in hopes that this will cause the mechanical response from the cartilage to increase roughly linearly, effectively increasing the pressure on the output electrodes and thereby multiplying the output voltage by an equal amount. However, the cross-talk phenomenon again becomes an argument against this idea because one cannot tell if an increase in the output is due to an actual increased mechanical pressure or to more voltage being leaked through from the input electrodes to the output electrodes. In addition, if cross-talk were for instance primarily triggered by a certain threshold build-up of charge, increasing the input current would only bring on the onset of cross-talk that much faster. On the other hand, experimenting with this method has shown in the past that going up to a factor of three times the normal input current density has increased the output signal by some amount, while tests for cross-talk did not reveal any significant increases in the non-cartilage signals. However, the output signals themselves seemed somewhat less than optimal, in that they did not appear particularly sinusoidal or even strictly periodic, especially at the higher frequencies.

Another possible approach to this issue is along the lines of a minor modification to the probe structure. Specifically, it might be reasonable to use a thicker version of the piezoelectric PVDF film, which in theory would potentially give a proportionally

higher output voltage. This idea has only been considered as an option, and has not been pursued by any means. If the SNR issue becomes as much of a problem as the cross-talk phenomenon for hhv5.0, then it may well be worth the effort to give this approach closer study.

Chapter 4

Experimental Methods and Results

This chapter will present the methods used to conduct measurements of current generated stress using the hand-held probe. The goal of this chapter is to familiarize the reader with practical concerns and issues that can occur during a typical measurement.

4.1 Calibration

The procedure for calibrating hhv5.0 is straightforward. Calibration begins by loading the assembled probe into a Dynastat mechanical spectrometer, which allows the user to proscribe a specific load or displacement on a given object. The probe shaft is inserted and secured into a metal colette which is connected to a load cell. Directly centered below the probe is a porous rubber disk placed on a plexiglass chamber, as shown in (Figure 4-1).

After making the proper adjustments to the Dynastat, a static load of 50 kPa (80 g for the active surface area of hhv5.0) is proscribed and is achieved as the load cell lowers the probe so that the active face presses against the rubber disk. Once the static load has been applied, the proper connections must be made between the

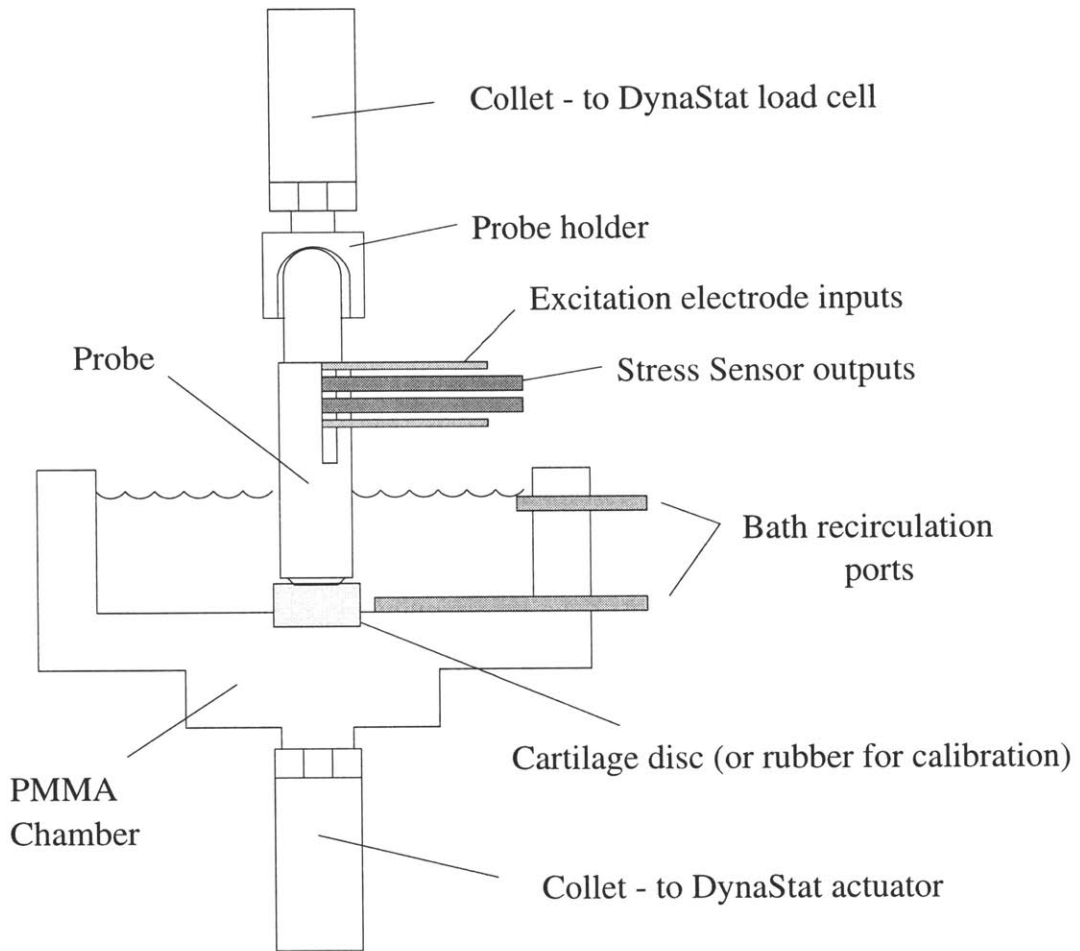


Figure 4-1: Setup for probe calibration and in vitro testing.

various hardware components required for the calibration system (Figure 4-2).

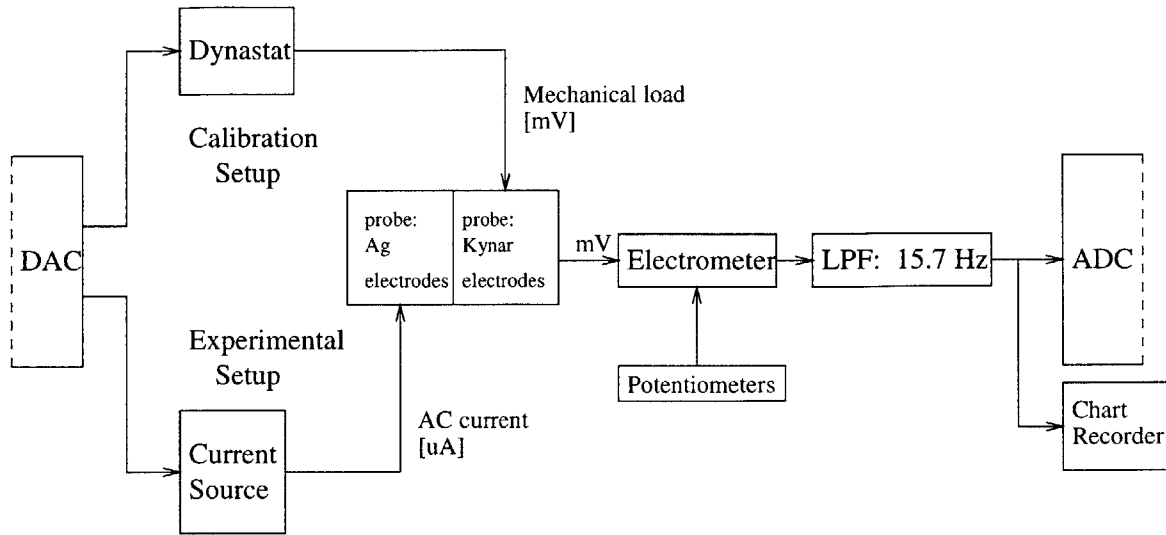


Figure 4-2: Connections for the calibration and experimental setups.

The software that controls the Dynastat load and displacement is then accessed, and is programmed to apply a dynamic sinusoidal load of a given amplitude over a range of frequencies. Typically, the probe is calibrated with a dynamic amplitude of 10 kPa (16 g) and 2.5 kPa (4 g) over the frequencies 1, 0.5, 0.25, and 0.1 Hz. It is interesting to note that in the past, the calibration frequencies have also included 0.05 and 0.025 Hz, but those frequencies have been discarded due to signal-to-noise issues. A more thorough discussion of noise issues can be found in Chapter 3.

After the computer has been set up, preparations are made to acquire calibration data by first starting the chart recorder and unshorting the Kynar output electrodes. Once the output electrodes are unshorted, the chart recorder shows an initial transient followed by a slowly varying voltage fluctuation originating from the piezoelectric electrodes. This low-frequency voltage swing is caused by the piezoelectric material reacting to minor pressure and temperature variations in its immediate environment, and is commonly referred to as drift. To account for the drift, a potentiometer is used to manually adjust the voltage so that it runs as close to zero as possible for each channel. Once the output voltages appear to be stable, the computer input is

initiated and the Dynastat proceeds to apply the particular dynamic loads at the required frequencies. If necessary, the pots may be used in between input cycles to re-zero the voltage.

Because the electrometer that is currently in use was originally intended for hmv4.0, it is capable of dealing with only two input signals at a time. This usually requires that the calibration procedure be repeated once so that all four piezoelectric output electrodes can be calibrated.

One comment that should be said about calibration is that it can be conducted either with or without the presence of fluid in the chamber. From observation, calibration numbers from both conditions are not significantly different from one another, but it is sometimes a useful check simply to see if there might be fluid leaking through the RTV silicone sealant. In such a case, the calibration would be expected to show no output voltage because the electrodes would be shorted to ground by the fluid.

4.2 Experimental Procedure

As with the calibration, the experimental procedure is also fairly straightforward. The initial steps involve setting up the appropriate wiring as was shown alongside that of calibration (Figure 4-2). Once the proper connections have been made, the probe face is immersed in the same solution that will hydrate the cartilage. As the probe sits and equilibrates to the temperature and pressure of the solution, the computer is set up to deliver a sinusoidal input current with current density $J = 1 \text{ mA/cm}^2$ at the same frequencies that were applied during calibration. Once the computer is set, both input and output electrodes are unshorted and the potentiometers may once again be used to compensate for the drift. The computer is initiated and proceeds to drive current from the silver electrodes into the solution. The data that is acquired is considered a measure for an undesirable phenomenon known as cross-talk, which is addressed in the Chapter 3.

After the cross-talk test has finished, the cartilage of interest is secured in an aluminum chamber, hydrated with solution, and brought to the probing area. The probe is then inserted into a cylinder containing a spring which has been pre-tested to give the correct static stress offset for the probe (Figure 4-3).

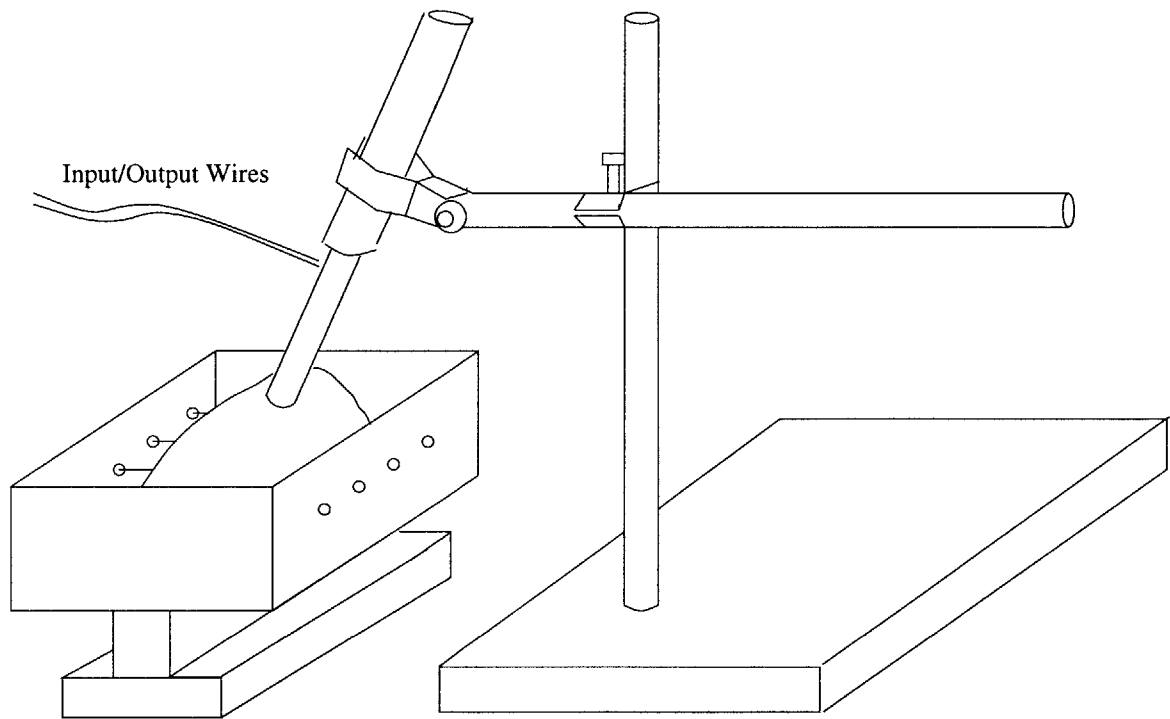


Figure 4-3: Typical setup for probing an intact joint.

At this point, it is very important to find a flat surface to place the probe on the cartilage. Once this has been done and checked, the probe is allowed to relax anywhere from 15 minutes to half an hour in order to readjust the probe to temperature and

pressure changes in its environment. The rest of the procedure then identical to that described for obtaining a measure of the cross-talk, and the data that is acquired is a measure of the current-generated stress normalized for each frequency, known also as normalized stress amplitude (NSA).

This cycle is repeated as many times as is desired, generally taking cross-talk measurements periodically between experimental cycles to check to make sure there is no observable signal during cross-talk measurements.

4.3 Validation Experiment

The following data was obtained from an experiment aimed at testing how long a particular hhv5.0 probe could obtain data before succumbing to cross-talk. In an attempt to maximize the use of the probe, parasitic tests were made only after every series of long and short data were taken.

Calibration for this probe showed that the PVDF electrodes were less responsive than on average. Average calibration numbers for PVDF electrodes of this size tend to be on the order of a 300 to 500 $\mu V/kPa$. Figure 4-4 show that the calibration numbers for these electrodes were mostly on the order of 200-300 $\mu V/kPa$. In the case of channel 1, the output was particularly low and very close to the noise floor.

Because of the calibration, a decision was made to use channel 1 as a control in the event that cross-talk occurred. Channels 2 through 4 would be used, two at a time, to test short and "long" wavelengths. Specifically, the short configuration would be tested with channels 2 and 3, and 3 and 4. While not technically long as previously defined, channels 2 and 4 would be used to approximate that wavelength.

After calibration, the calf patella to be tested was taken and secured in the aluminum holder (Figure 4-3). The entire patella was submerged in phosphate buffer solution (PBS) in order to keep the ECM hydrated. The probe was then placed on a

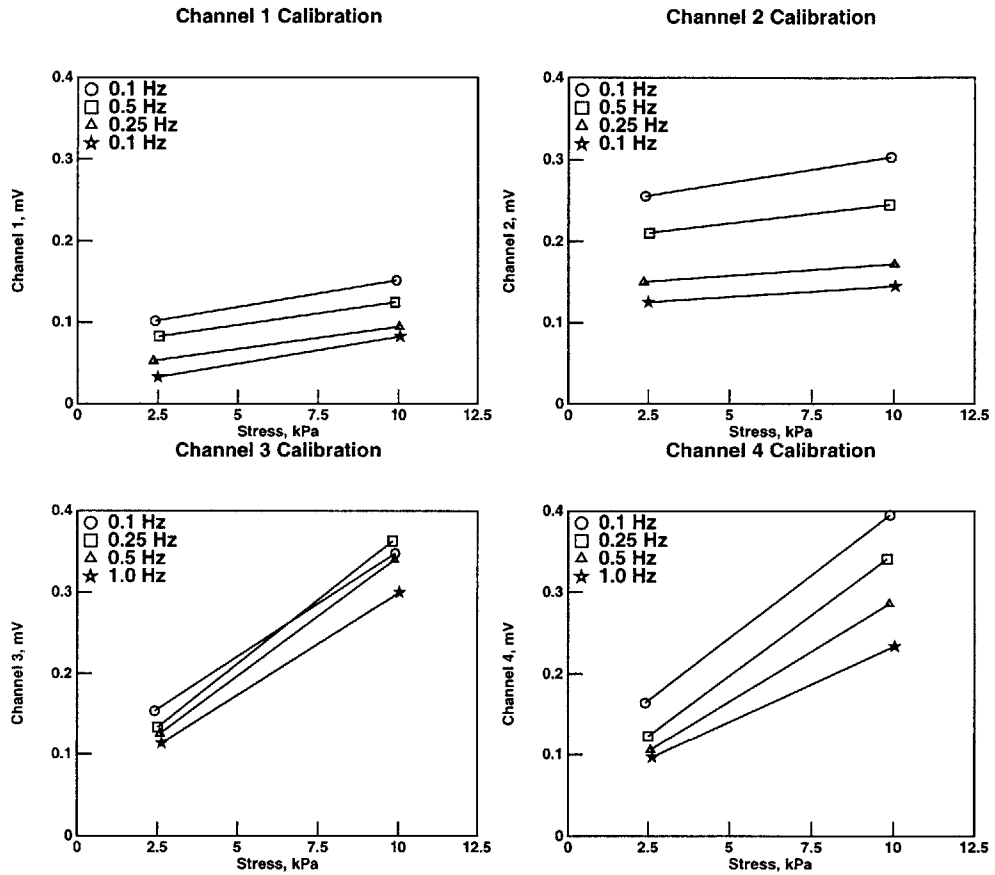


Figure 4-4: Calibration plots for validation experiment. Note that channel 1 is particularly low compared to channels 2 through 4.

flat surface of the patella in a spring-loaded holder which held the probe surface at a stress of 50 kPa. The probe and patella were allowed to equilibrate for 30 minutes.

The first series of tests involving the short configuration with channels 2 and 3 were then conducted, using current density $J = 1 \text{ mA/cm}^2$ and frequencies 1, 0.5, 0.25, and 0.1 Hz. After testing, the probe was pulled off the patella and allowed to hang freely in the PBS solution in order to obtain a cross-talk test. This cycle was then repeated for another short configuration with channels 3 and 4. The top two plots in Figure 4-5 show that the averaged amount of normalized stress is fairly consistent with either short configuration, and that the amount of cross-talk is generally lower than the signal from a cartilage test. Note that at the upper frequency values, the cross-talk can approximate or even exceed the signal from actual cartilage.

The cycle was repeated once more for the "long" configuration with channels 2 and 4, as shown in the lower left-hand plot of Figure 4-5. During the "long" test, there was a marked increase in the amount of signal, which suggested either a very good CGS signal from cartilage, or the onset of cross-talk. A cross-talk test revealed that a signal virtually indistinguishable from that of cartilage CGS occurred even in pure PBS solution, indicating that the cross-talk effect had occurred.

Once the cross-talk occurred, the configuration was switched back to short, with channels 1 and 2 as the testing electrodes. Both a cross-talk and cartilage test were done in order to see if both tests would yield similar results. The lower right-hand plot of Figure 4-5 shows that the results were indeed fairly similar, suggesting that channel 1 had been affected by the cross-talk effect even though it had not been used to drive current into the cartilage.

The results of this validation experiment illustrate a number of issues that currently characterize hhv5.0. The first issue is that of probe lifetime. In this instance, the probe was used to run cartilage and cross-talk tests a mere 6 to 8 times before cross-talk appeared. While cross-talk appeared in this particular experiment relatively

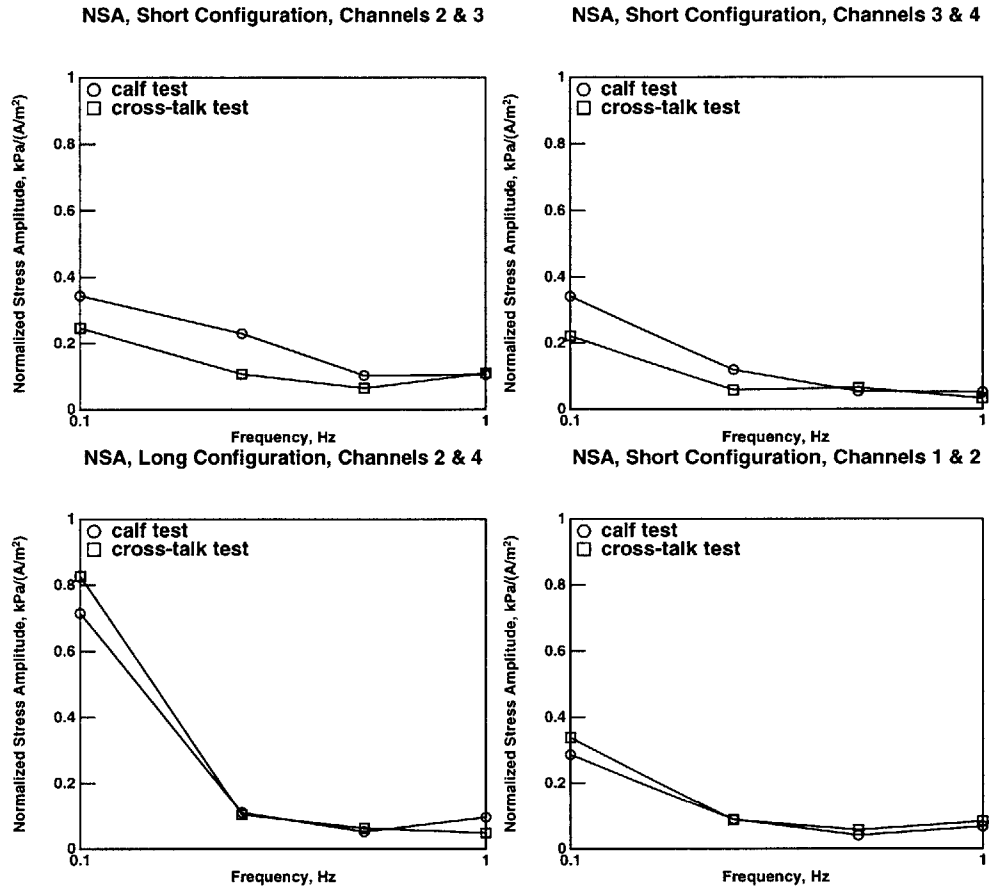


Figure 4-5: Experimental results of validation experiment. Note that cross-talk tests were generally lower than the calf tests for the plots of short configuration 2 and 3, and 3 and 4. However, the cross-talk tests were comparable in value to the calf tests in the plots for the long configuration and for the short configuration 1 and 2, showing that cross-talk had set in.

quickly, the time of onset in the past has generally been longer, but has always occurred without warning. It is somewhat interesting to note that channel 1 was also affected by the cross-talk phenomenon, even though that particular electrode had not been used to drive current at all. This suggests that the cross-talk effect marks some sort of punch-through effect across the entire Mylar ground plane, rather than a localized effect between each silver and piezoelectric electrode. Thus, this supports the theory that cross-talk is indeed a capacitive phenomenon, and that efforts to improve the shielding between the sets of input and output electrodes might be a logical next step in the effort to eliminate cross-talk.

Chapter 5

Summary and Discussion

The diagnostic probe hhv5.0 presented in this thesis has exciting potential for quantitatively and semi-invasively determining the health of cartilage. Previous and current work done on the probe has involved validating the basic theory behind the probe and testing the theory with experimentation on various types of cartilage [10, 4, 12, 1, 13, 2]. The next step in the evolution of hhv5.0 is to establish and maintain the consistency of the probe from one experiment to another, and to finalize the supporting software and peripheral hardware necessary for the use of the probe *in vivo*.

To accomplish these goals, a few specific issues remain as major obstacles that need to be overcome. The first and foremost issue is the reliability of the PVDF piezoelectric film. While several suggestions as to how to improve the reliability and lifetime of each probe have been presented in this thesis, the fact remains that there is currently a general lack of expertise on the issue of environmental variables that can potentially alter or even damage the piezoelectric film. Many related issues, including the currently mysterious capacitive cross-talk, the variability of the piezoelectric electrodes (both from pad to pad on each probe and from probe to probe), and the signal-to-noise ratio, would undoubtedly benefit from a deeper understanding of the electromechanical material properties of the piezoelectric film.

The second major issue facing the probe project is that of the supporting software and peripheral hardware. The peripheral hardware has essentially been successfully designed and tested. What remains to be done is to combine the hardware with software which can display and record probe data during a calibration run or an experiment, and which can control the voltage drift of the piezoelectric electrodes. In the past, a custom-written software package has been sufficient for recording calibration and experimental data. However, with the recent increase of electrodes from two to four on hhv5.0, it has become necessary to abandon the old software package in favor of commercially available Labview. This approach has the advantage of allowing probe users to dynamically monitor an arbitrary number of input and output channels *in time*, but has the disadvantage of requiring both calibration and experiment procedures and functions to be rewritten in an unfamiliar software package. While this upgrade will take some time, the end result should be a more powerful and ultimately more flexible system for applying surface spectroscopy to cartilage.

Once these obstacles have been overcome, the final hhv5.0 system will be in a state with many possible options. One of the most immediate and attractive options would be to make the hhv5.0 commercially available to surgeons performing arthroscopies, an option that already has the interest of several parties. Another natural option would be to apply the probe to further study of cartilage biomechanics, including animal models (e.g. canine, bovine). One other option would be to apply the probe to study of materials other than cartilage which are composed of substrates with fixed-charges and free-floating charges (e.g. semiconductors). At this stage, the possibilities and opportunities for this system should be quite broad.

Bibliography

- [1] S I Berkenblit. *Spatial Localization of Cartilage Degradation Using Electromechanical Surface Spectroscopy With Variable Wavelength and Frequency*. PhD thesis, Massachusetts Institute of Technology, 1996.
- [2] D L Bombard. A surface probe for *in situ* detection of cartilage degradation via electromechanical spectroscopy. Master's thesis, Massachusetts Institute of Technology, Cambridge, MA, 1995.
- [3] M Doherty. *Color Atlas and Text of Osteoarthritis*. Times Mirror International Publishers Limited, London, 1994.
- [4] E H Frank, E P Salant, and A J Grodzinsky. Nondestructive surface detection of cartilage degeneration based on electromechanical behavior of extracellular matrix. 16:74, 1991.
- [5] K E Kuettner and V M Goldberg. *Osteoarthritic Disorders*. American Academy of Orthopaedic Surgeons, 1995.
- [6] T Lyyra, J Jurvelin, P Pitkänen, U Väättäinen, and I Kiviranta. Indentation instrument for the measurement of cartilage stiffness under arthroscopic control. *Medical Engineering and Physics*, 17:395–399, 1995.
- [7] T Minas and S Nehrer. Current concepts in the treatment of articular cartilage defects. *Orthopedics*, 20(6):525–538, June 1997.

- [8] R W Moskowitz, D S Howell, V M Goldberg, and H J Mankin, editors. *Osteoarthritis: Diagnosis and Medical/Surgical Management*. W.B. Saunders, Philadelphia, 2nd edition, 1992.
- [9] C A Poole. The structure and function of articular cartilage matrices. In J F Woessner, Jr and D S Howell, editors, *Joint Cartilage Degradation*, chapter 1, pages 1–35. Dekker, New York, 1993.
- [10] J R Sachs. *A Mathematical Model of an Electromechanically Coupled Poroelastic Medium*. PhD thesis, Massachusetts Institute of Technology, Cambridge, MA, 1987.
- [11] J R Sachs and A J Grodzinsky. An electromechanically coupled poroelastic medium driven by an applied electric current: surface detection of bulk material properties. 11:585–614, 1989.
- [12] E P Salant. *Surface Probe for Electrokinetic Detection of Cartilage Degeneration*. MD thesis, Harvard-MIT Division of Health Sciences and Technology, Cambridge, MA, 1991.
- [13] S Treppo. *Physical Diagnosis of Cartilage Degeneration*. PhD thesis, Massachusetts Institute of Technology, Cambridge, MA, 1999.